Validation of Power System Control Methodologies using a Microgrid Testbed Employing Low and Medium Voltage AC and DC Sources

C. Tschritter*, A.N. Johnston*, L. Vuʕ, T. Nguyenʕ, D.A. Wetz*, T.V. Vuʕ, K. Schoderǂ, J. Langstonǂ, H. Ravindraǂ, M. Stanovichǂ, C.M. Schegan+, and J.M. Heinzel+

* *Univ. of Texas at Arlington (UTA), Arlington, TX USA*
ʕ *Clarkson University, Potsdam, NY USA*
ǂ *Florida State University, Center for Advanced Power Systems, Tallahassee, FL USA*
+ *Naval Surface Warfare Center - Philadelphia, Philadelphia, PA USA*
* Corresponding Author. Email: wetz@uta.edu

Synopsis

Future shipboard power systems are likely to look and operate much differently than they do today. The changes stem from the need to operate a much wider array of loads, many of which will demand high power in a transient manner. Architectures employing distributed power generation sources and energy storage are attractive, especially when the hooks are built in to rapidly control as many facets of the sources and loads as possible. This however is not always possible as more flexibility comes with increased complexity and costs that are not always easy to implement. As control strategies are developed, testbeds are needed to validate simulations and performance when real hardware is involved. Here a low and medium voltage (MV) AC and MV DC testbed at the University of Texas at Arlington (UTA) is being used to study robust control algorithms that are being developed and modeled by Clarkson University (CU). The testbed emulates one zone of a multi-zone power system and CU has developed algorithms intended for optimized shedding of loads and the ramp-rate support of a generator supplying transient loads. Multiple levels of control have been introduced to study the impact each has on maintaining power system operability. The testbed and its integration with these control strategies will be presented along with experimental results collected to date.

Keywords: Power System Control, Energy Storage, Load Shed, Ramp-rate, Pulsed Loads

1. Introduction

In 1903, the first diesel electric ship, the Vandal, was launched into the water. At the same time, another ship utilizing diesel electric propulsion, the Petite-Pierre, was launched as well. By the 1920s ships using diesel electric propulsion were being mass constructed. These ships generally employed steam-based turbine generators to drive the propeller motors and the speed of the motor is adjusted through the speed of the generator (Hansen 2015). This

 https://doi.org/10.24868/11152

class of shipboard power systems started to fall to the wayside however with the introduction of diesel engines. The all-electric concept did stage a resurgence in the 1980s due to the advancement of power electronic devices and the concept accelerated with the increased viability of variable speed drives in the 1990s (Ortiz 2010). An abundance of studies covering shipboard power system architectures employing medium voltage (MV) AC, MV DC, or some mixture, have been conducted with progress gradually being made suggesting expanded usage soon. Many cruise vessels liquefied natural gas (LNG) tankers, and icebreakers, currently employ electric propulsion, as well as AC and DC loads in constant or transient operation (Office of Naval Research 2021). These ships and studies have highlighted the benefits of a microgrid architecture; however, considerable work and study is still necessary for these architectures to reach their full potential. The work presented here is a stride to reach the full potential of this architecture.

Among the advantages a microgrid architecture offers are improved operability and reduced susceptibility to power quality issues that occur when transient loads are deployed. The ability to actively control multiple sources and shed lower priority loads significantly improves the operability. Load shedding should occur quickly when there is not enough power to source all the loads, ensuring that critical loads remain powered (Doerry 2010, Tschritter 2023a, Johnston 2022). Without real-time control and monitoring, load shed events could happen randomly and with zero consideration of priority or operability. When monitoring and controls are available, loads may be shed in a controlled manner, offering the ability to prioritize and maximize operability of the system. When transient loads are ramp-rate buffered using energy storage, the voltage and frequency sags and surges are significantly reduced, greatly improving power quality. Without active ramp-rate buffering, the heavy loading and unloading of traditional generation sources occurs uncontrollably with detrimental impact on the generator efficiency.

Here, the University of Texas at Arlington (UTA), will demonstrate the deployment of transient loads on a low and MV AC and DC testbed known as the Intelligent Distributed Energy Analysis Laboratory (IDEAL) (C. Tschritter, 2022, C. Tschritter, 2023, C. Tschritter, 2024, A.N. Johnston, 2020, A.N. Johnston, 2020, A.N. Johnston, 2021, A.N. Johnston, 2022). Recently a 37-kW diesel generator was integrated into the testbed and it is able to be operated alone and in synchronization with the other generators in the testbed using a Woodward ATLAS-II™ generator controller. This work will be presented. A demonstration of Clarkson University's (CU's) Advanced Load Shed (ALS) and Predictive High Ramp-Rate (PHRR) controls, which have been previously documented in (C. Tschritter, 2023 and C. Tschritter, 2024) will also be made.

IDEAL Experimental Testbed

The IDEAL testbed has been documented extensively in previous work, as referenced above, but it is always changing and growing. To reduce the repeat of previously published work, the readers are referred to those articles for a more thorough understanding. The purpose of the IDEAL testbed is to emulate a single zone of a distributed shipboard zonal power system architecture. Zonal architectures for shipboard power systems have been previously proposed as seen in Doerry's one-line diagram in Figure 1 (Doerry 2010). The IDEAL testbed employs multiple sources and loads that are monitored and controlled to demonstrate the benefits these features afford towards improving operability and power quality, among other metrics.

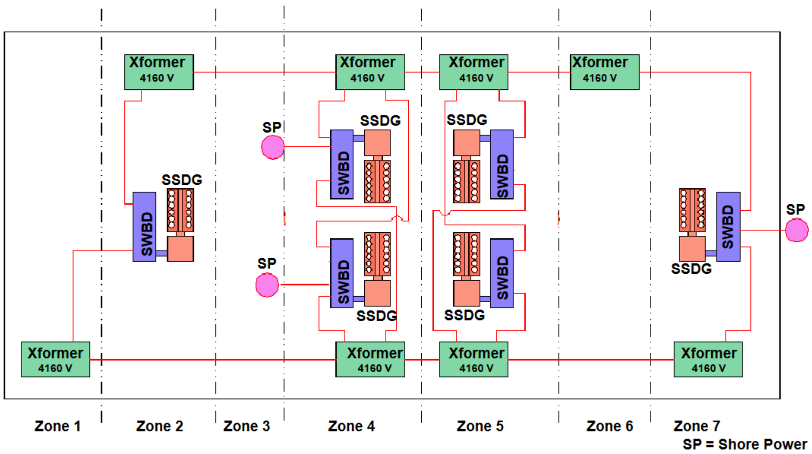

Figure 1. One line diagram depicting a potential zonal organization of shipboard power systems.

A one-line diagram of the IDEAL testbed is seen in Figure 2. In the upper left-hand side of the diagram, two generators are seen. The first is the 37 kW diesel generator previously mentioned. The second is a 150-kW electric motor generator that is controlled by a variable frequency drive. The two generators can be operated independently, or they can by synchronized using a Woodward ATLAS-II™ engine controller. Off the 480 VAC bus, there are multiple continuous and transient loads employed. The first is ~200 kW MV power electronic drive that produces a three phase, 4160 VAC output. Its output is split two ways. In the first, it is transformed back down to 480 VAC and fed into a 350-kW resistive load bank that is digitally broken up into multiple smaller loads, referred to as Non-Vital Load L1-1 and Non-Vital Load L2-2. The second is into a multipulse rectifier that produces a 6 kVDC output that is connected to a three step, 50 kW each, resistive load bank. That load is broken up into Vital Load L2-1 and Non-Vital Load L2-2. Next the 480 VAC bus is loaded by a power supply that creates 0 – 12 kVDC at 0 – 8 A. Its output current is adjusted using an analog reference voltage from the controller to emulate continuous or transient load(s) using another resistive load. Here that load is broken up into Vital Transient Load L3-1 and Vital Transient Load L3-2. Next, there are two power electronic converters that interface the 480 VAC bus to a DC bus operating between 750 VDC and 1000 VDC. Here, only one of the converters is used, the 150 kW AC/DC converter, that is unidirectional from AC to DC. It creates 0 – 1200 VDC at 0 – 125 A. It output current is adjusted using analog controls to force power from the generator(s) onto the DC bus. The second converter is a bi-directional supply that allows power to be transferred from the battery on the DC bus back up to the L1, L2, and L3 group loads but again it is not employed in the work presented here.

On the DC bus, there are multiple devices connected. On the left side there is a 40-kW electric motor-generator set that produces a nine-phase, 711 VAC output that is rectified using an actively controlled AC/DC rectifier onto the DC bus. That generator set is not employed in the work presented here. There is also a 500-kW bi-directional power converter between the main building grid and the DC bus that can be used to emulate sources or loads as needed but that is also not used here. On the right side, there is a resistive Mission Load 1 (ML1) that is sourced by a DC/DC converter that creates 0 – 6 kVDC at 0 – 12.5 A. The supply's output current is regulated using an analog reference signal from the controller. Finally, there is a lithium-iron-phosphate (LFP) battery that is floated on the DC bus to buffer the generator when the transient ML1 is operated as described later.

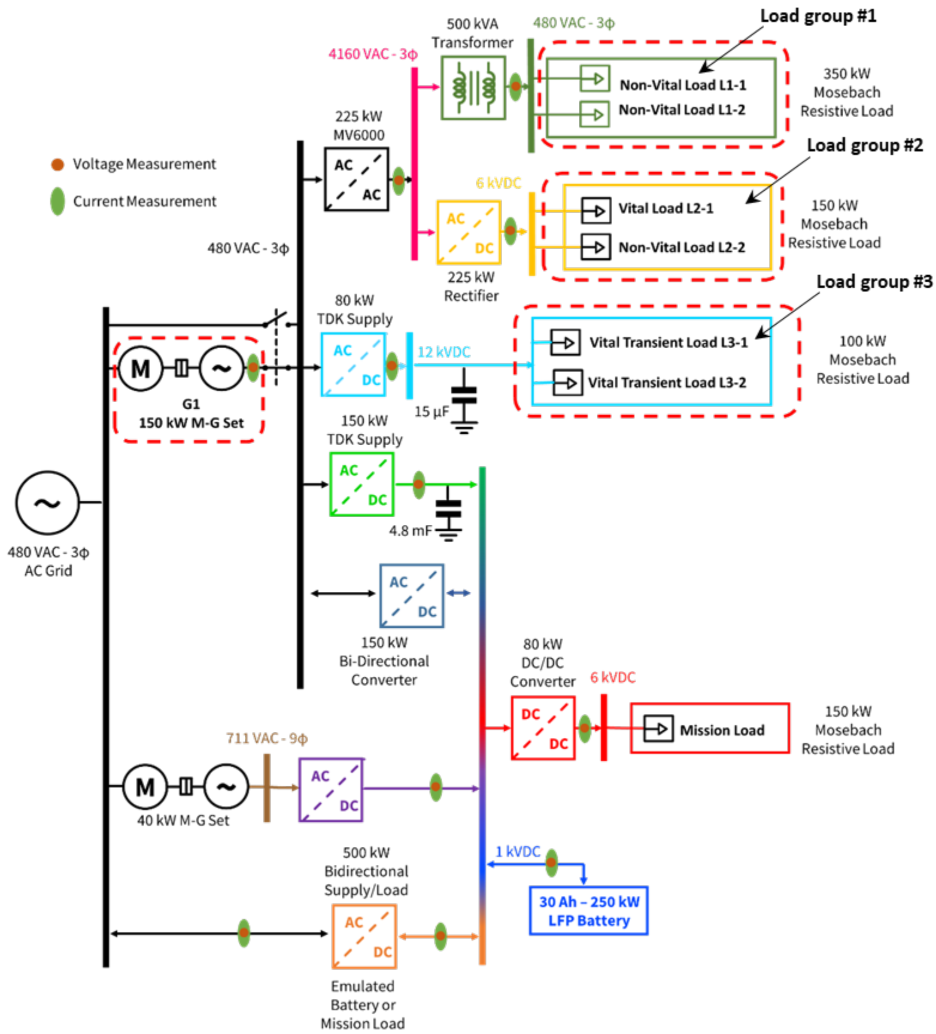

Figure 2. One Line diagram of the Intelligent Distributed Energy Analysis Laboratory (IDEAL) hardware.

 https://doi.org/10.24868/11152

A critical addition to the testbed is the 37-kW diesel generator (DG). The importance of the DG is highlighted as it more effectively represents a shipboard diesel generation as compared to the 150-kW electric motor generator (MG) set. The diesel allows for a more realistic measure of power quality when transient loads are supported and the impact adjusting its ramp-rate while buffered by energy storage can improve it. Ramping of the generation source through buffering by energy storage along with the impact transient loads have on power quality are more accurately represented when using the diesel generator. Because this generator is sized for 37 kW, all the loads have been scaled to create similar impact as compared to using the MG set. In this scenario, the loads L2-1 and L2-2 are unable to be used since they require a minimum of ~45 kW each. Instead, they are emulated by splitting the resistive load bank that represents L1-1 and L1-2 into four loads. This change makes no noticeable difference to the power architecture.

When multiple generator sets are employed in a shipboard power system, they must be synchronized such that their voltage waveforms and frequencies are aligned before they can be tied onto the same bus. This is achieved using an engine-generator controller, in this case a Woodward ATLAS-II™. On its own the ATLAS-II™ can synchronize and close the breakers on two generators but when a third generator is added, additional hardware is needed. Here Woodward LS5 breaker controllers are installed on each of the three 480 VAC generators. The ATLAS-II™ brings the generators into synchronization and works with the LS5s to physically connect the generators onto the bus when the time is right. The dual wound generator was only recently installed, after the work discussed here was performed, so synchronization of only the DG and MG will be discussed here. Together, they bring the total power capability of the testbed up to 187 kW. A one-line diagram showing the ATLAS-II™'s integration with the LS5's in the testbed is shown in Figure 3.

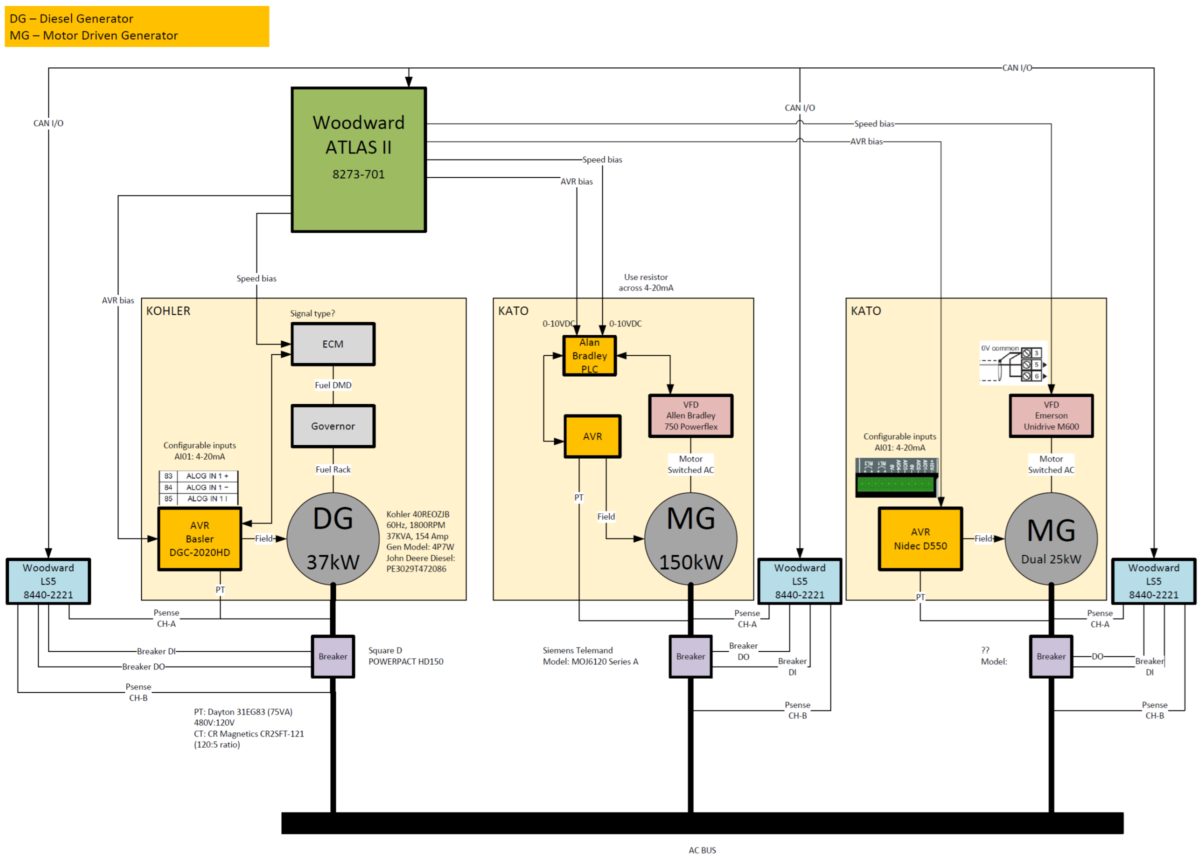

Figure 3. One Line diagram of ATLAS II connecting the 150 kW MG and 37 kW DG.

2. ALS and PHRR Control Methodology

Two software controllers, known as the ALS and PHRR controllers, have been developed by CU and deployed to the IDEAL testbed. In 2023, a series of experiments were performed using only the MG set as a source and it was demonstrated how successful the ALS and PHRR controls were at improving operability and ramp-rate support of the MG set (Tschritter 2023a, Tschritter 2023b). The ALS and PHRR were described in detail in those prior publications and the reader is referred to those for more in depth understanding. In summary, the ALS controller keeps the load demand below the generation capacity shedding the lowest priority loads when necessary

 https://doi.org/10.24868/11152

to ensure maximum operability. The PHRR controller's primary purpose is to improve and maintain power quality during the operation of transient loads. The PHRR controller achieves this by regulating the current, and therefore the power, supplied by the 1 kV converter. By doing this, it forces the battery to buffer the ML and allows the generator to be ramped on and off as transient loads come on and off the bus. This decreases the deviations on the voltage and frequency of the generator's 480 V bus when operating transient loads. Figure 4 presents a diagram showing how the IDEAL testbed interfaces with CU's ALS and PHRR controls that run on a Simulink Real-Time computer. The two systems communicate via User Datagram Protocol (UDP) messaging with delay times on the order of 100 ms.

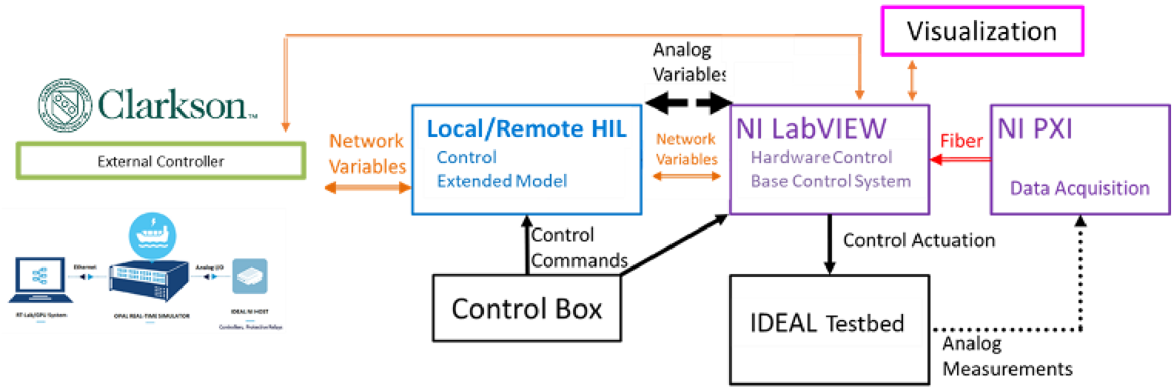

Figure 4. Flow diagram of Clarkson's controller integrating with the NI controller and IDEAL.

3. Experimental Results

3.1. *Transient unbuffered loading*

Multiple experiments have been conducted here to assess the power quality of the 480 V bus when transient loads are deployed. Military Standard (MIL-STD) 1399 specifies the power quality limits for a 440 V 60 Hz generator. Figure 6 and Figure 7 plots the voltage and frequency envelope limits defined in MIL-STD 1399. These specifications do not specify standards for a 480 V system, but to provide an appropriate measure for the scenarios tested here by scaling the 440 V standard to 480 V, making the line-to-line root-mean-square (RMS) voltage bounds used for this demonstration 446 V and 504 V.

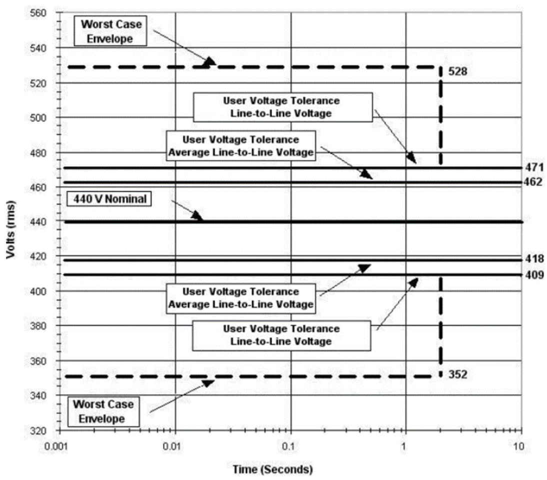

Figure 5. Voltage power quality standard from MIL-STD 1399.

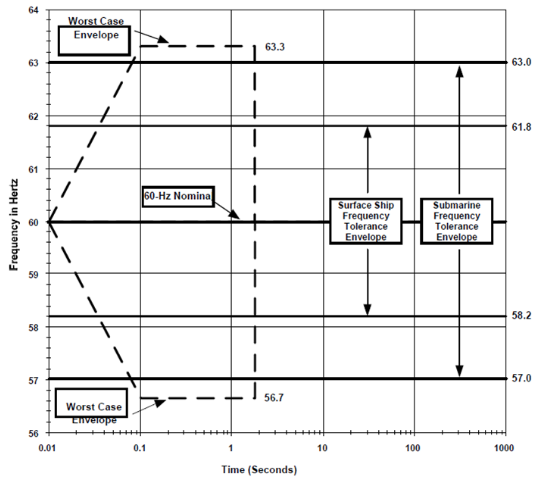

Figure 6. Frequency power quality standard from MIL-STD 1399.

To characterize when the DG's voltage and frequency deviations exceed the power quality standards, a 10 second step load was engaged and disengaged, incrementing the load by 10 kW on each subsequent engagement until it reaches 40 kW. Figure 7 and Figure 8 present voltage and frequency measurements collected from the DG during the four respective transient load events. As seen in the figures, the frequency deviation exceeded the worst case bound of 56.7 Hz when the step load power reached 30-kW step load. The 20-kW load is also outside MIL-

STD 1399 due to the recovery from the worst case bound on the frequency to the standard bound taking longer than 2 seconds to recover.

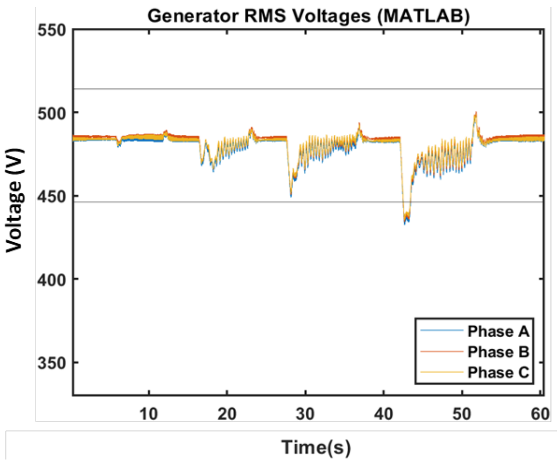

Figure 7. Voltage deviation as transient load increases.

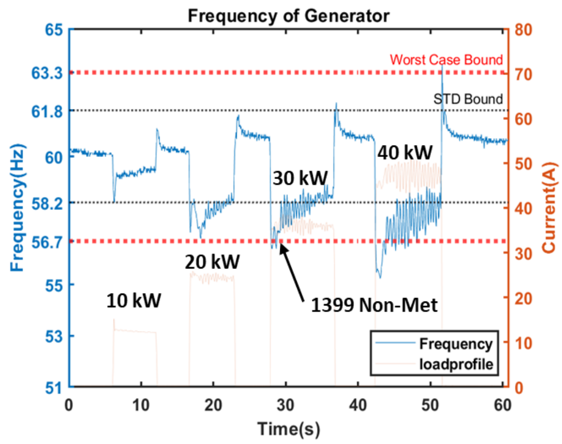

Figure 8. Frequency deviation as transient load increases.

3.2. Ramp-rate and power quality improvement

Since the MIL-STD 1399 frequency bounds were exceeded when it was transiently loaded with a 30-kW step, that power level is used in subsequent load scenarios to identify how the PHRR improves the power quality metric. Because the voltage of the DG set was maintained within the standard bounds during the 30-kW load while the frequency failed, improving frequency is the primary focus. Figure 9 presents data collected when the generator was ramped through the 1 kV DC power converter at rates of 2 kW/s, 4 kW/s, and 8 kW/s up to 30 kW. As shown, only the 2 kW/s ramp-rate kept the generator fully within the bounds of MIL-STD 1399. In the 4 kW/s and 8 kW/s plots, the cyan lines indicate the 2-second recovery window specified by the MIL-STD 1399. In those cases, the frequency does not recover to within the standard bounds within the 2 second envelope. This means that 2 kW/s is a safe ramp-rate as high as 4 kW/s can be used in extreme conditions where power quality is less paramount.

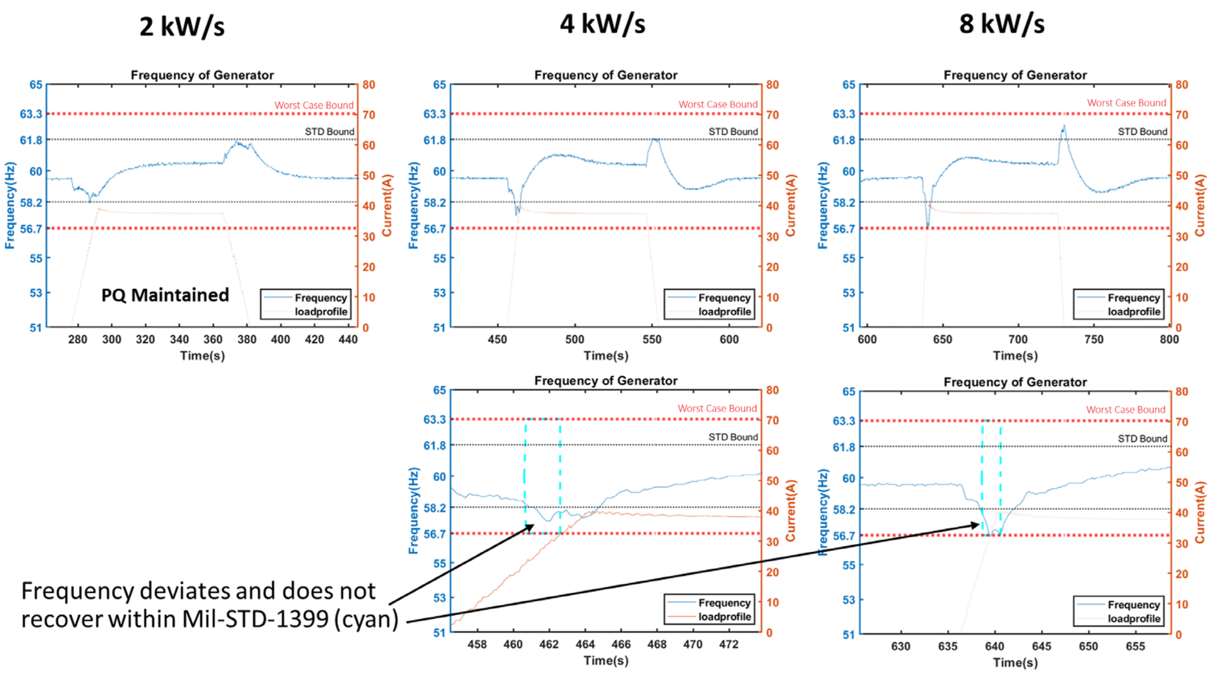

Figure 9. 4 kW/s constant ramp of a 30-kW load.

 https://doi.org/10.24868/11152

3.3. PHRR results

The ramp-rate values above were provided to CU for consideration in their development of their PHRR algorithm. The PHRR controller uses the 4.4 kW/s ramp-rate as an upper bound, meaning the ramp-rate will typically be lower, but can be pushed to the upper bound. To demonstrate the PHRR controller, a repeated load profile of 32 kW was engaged and disengaged in a 5 second on, 1 second off profile. This repeated program is stressful on the DG and provides several opportunities for the power quality to falter. At the start of each pulse, the transient load is initially buffered entirely by the battery, and then the generator is ramped up at a rate of 4 kW/s. This is repeated for 10 engagements, with the generator current being maintained through the off periods while it recharges the battery. Upon completion of the tenth load cycle, the current continues to recharge the battery until its state of charge (SoC) reaches 60%. A graph plotting the power sourced by the battery, the load power through the 6 kV AC/DC power converter, and the power supplied by the generator through the 1 kV AC/DC converter converter, is seen in Figure 10. Additionally, a graph of the frequency deviation is included in Figure 11, which demonstrates full compliance with MIL-STD 1399.

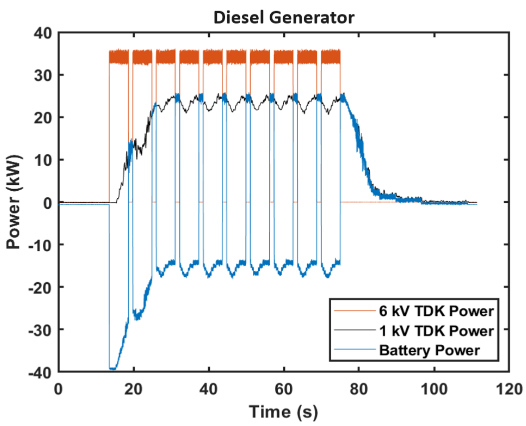

Figure 10. PHRR controller with a 4 kW/s max ramp-rate.

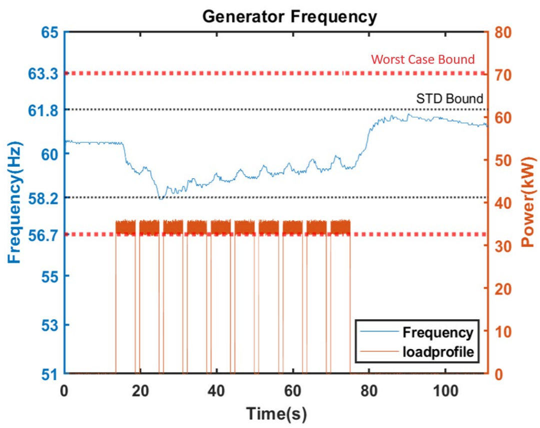

Figure 11. Frequency deviation during the PHRR controller scenario.

3.4. Generator Failure

To emphasize the importance of load shed algorithms, a scenario utilizing synchronized generators is shown. In this scenario, a generator failure is emulated by opening a breaker on one of the generators, causing the load demand to exceed the generation capacity of the system with no load shed intervention. Figure 12 shows the power and frequency behaviour of each generator across the test time. The two generators in the system are synchronized together with a 60-kW base load between them at approximately the 30 second mark. The dashed blue line represents the power sourced from the MG set with a maximum rating of 150 kW. The power sourced by the DG set is represented by the solid blue line and is has a maximum rating of 37 kW. After about 2.5 minutes, the MG set breaker is opened, causing the DG to become the only generation source. The power output is unable to be maintained by the DG alone, resulting in the bus voltage and frequency sagging. The sagged output of the generator continues for approximately 5 seconds, after which the LS5 breaker controller opens the DG breaker to protect it, ultimately resulting in all 60 kW of load failing to be supplied. This is one of the worst possible outcomes for the power system, with a silver lining of the DG being protected due to the LS5's intervention.

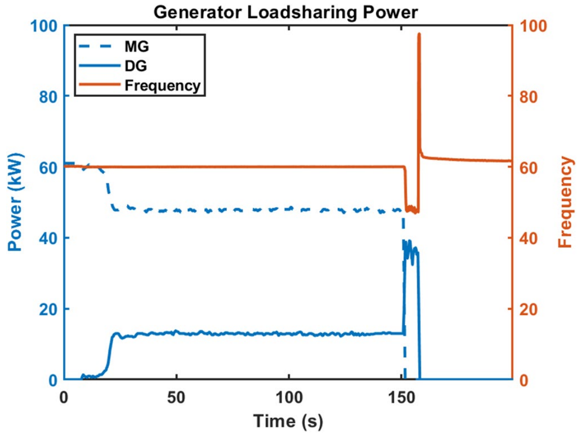

Figure 12. Scenario where loss of generator causes unintentional load shed.

3.5. ALS Controls on the Disel generator

In an effort to prevent the situation in the previous scenario, the ALS controller is deployed. A sample scenario showing the effectiveness of the controller is described here. After load is put onto the bus, the allowable power generation of the DG is manually reduced in the controller, causing the power being supplied to exceed that allowed by the controller. The breaker on the MG is not opened here, but the scenario effectively replicates generation loss, as well as other cases where a generator may become derated below nominal power. Table 1 presents each load's power ratings and weights. Figure 13 plots data collected during the generator derating scenario. Loads L1-1, L1-2, L2-1, L3-1, and L3-2 are engaged. At the 49 second mark, the generator is derated from its original 37 kW to 32 kW. This causes the ALS controller to shed L1-1 to bring the load demand below the power generation capacity. This maximizes the operability of the system, protects the generator, and prevents any uncontrolled load shed events from occurring.

Table 1. Load ratings and weights used for the DG

	DG Source	
Load	Rating (kW)	Weight
L1-1	4	0.2
L1-2	4	0.2
L2-1	8	1
L2-2	8	0.2
L3-1	8.5	0.5
L3-2	8.5	0.5
Gen	37	NaN
Reserved power	5%	NaN

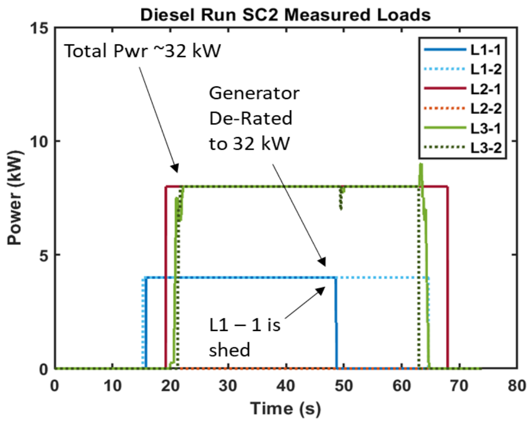

Figure 13. ALS scenario 2.

4. Conclusions

Future shipboard power systems are likely to employ a much wider array of loads, many of which will demand high power in a transient manner. The sudden high-power demands can have a detrimental effect on the entire power system. To mitigate these effects, new shipboard power system architectures propose the use and deployment of well monitored and controlled microgrid or zonal topology. UTA has setup a low and medium voltage AC/DC testbed on which to study these architectures along with the required monitoring and control strategies. In this work, a DG installed on the IDEAL testbed was used to demonstrate the power quality challenges that transient loads can introduce. ALS and PHRR controls developed by CU were implemented to improve operability when load shed events become necessary and maintain power quality when transient loads are employed.

Acknowledgements

The authors would like to thank ONR for their financial support of this effort through grants N00014-18-1-2714, N00014-21-1-2124, and N00014-21-1-2239. Any opinions and findings are those of the authors and not those of ONR or NSWC-Philadelphia

References

J.F. Hansen and F. Wendt, 'History and State of the Art in Commercial Electric Ship Propulsion, Integrated Power Systems, and Future Trends,' Proceedings of the IEEE | Vol. 103, No. 12, December 2015.

G. Ortiz, J. Biela, D. Bortis, J.W. Kolar, "1 Megawatt, 20 kHz, Isolated, Bidirectional 12 kV to 1.2 kV DC-DC Converter for Renewable Energy Applications," The 2010 International Power Electronics Conference – ECCE ASIA, IEEE, 2010.

ONR Electric Ship Research Development Consortium, https://www.esrdc.com/, Online August 19, 2021.

N. Doerry, 'Shipboard Distribution Systems: Present and Future,' CAPS 10th Anniversary Celebration & NGIPS Workshop, October 14-15, 2010, Tallahassee, Florida, http://doerry.org/norbert/papers/20101014CAPS-DistributionSystems-final.pdf

C. Tschritter, A.N. Johnston, T. Nguyen, D.A. Wetz, T.V. Vu, J. Langston, H. Ravindra, M. Stanovich, K. Schoder, C.M. Schegan, and J.M. Heinzel, 'Robust Control of a Medium Voltage AC/DC Testbed,' 2022 International Ship Control Systems Symposium (iSCSS), November 7 – 10, 2022, Delft Netherlands.

C. Tschritter, A.N. Johnston, L. Vu, T. Nguyen, D.A. Wetz, T.V. Vu, J. Langston, H. Ravindra, M. Stanovich, K. Schoder, M. Steurer, C.M. Schegan, and J.M. Heinzel, 'Advanced Load Shed and Predictive Ramp Rate Control of a Medium Voltage AC/DC Testbed,' 2023 IEEE Electric Ship Technologies Symposium (ESTS), August 1 – 4, 2023, Alexandria, Virginia

C. Tschritter, A.N. Johnston, L. Vu, T. Nguyen, D.A. Wetz, T.V. Vu, J. Langston, H. Ravindra, M. Stanovich, K. Schoder, M. Steurer, C.M. Schegan, and J.M. Heinzel, 'A Prediction and Load Shed Based Approach of Controlling a Medium Voltage AC/DC Testbed,' Journal of Marine Engineering Technology (JMET), https://doi.org/10.1080/20464177.2024.2340897, April 2024.

A.N. Johnston, Z.R. Bailey, D.A. Wetz, G.K. Turner, and J.M. Heinzel, 'Design and Commissioning of a Medium Voltage Testbed with Emulated Pulsed Loads,' Naval Engineers Journal, Volume 134, Number 3, 1 September 2022, pp. 129-144(16).

A.N. Johnston, G.K. Turner, D.A. Wetz, Z.R. Bailey, C. Schegan, J.M. Heinzel, and M. Giuliano, 'Emulation of a Single Zone of an Integrated Power System,' American Society of Naval Engineers (ASNE) Intelligent Ships Symposium (ISS), April 28 – 29, 2021, VIRTUAL.

A.N. Johnston, D.A. Wetz, R. Madani, A. Davoudi, G.K. Turner, D.A. Dodson, B.J. McRee, Z. Bailey, D. Pullaguram, J.M. Heinzel, M. Giuliano, and C.M. Schegan, 'Mitigating Transient Loads in Medium-Voltage Direct Current Microgrids,' Proceedings of the 2020 American Society of Naval Engineers (ASNE) Advanced Machinery Technology Symposium (AMTS), October 7-8, 2020, Philadelphia, Pennsylvania.

A.N. Johnston, D.A. Wetz, Z. Bailey, D.A. Dodson, B.J. McRee, and J.M. Heinzel, 'A Medium Voltage, Distributed Power Generation Testbed Deploying Transient Loads,' Proceedings of the International Ship Control Systems Symposium (iSCSS), October 6 – 8, 2020, Delft, Netherlands.